Mass Transport of Progressive Edge Waves : A Comparison between the Full and Shallow-Water Wave Theories

K. M. Mok[1] & Harry Yeh[2]
[2]Member of ASCE

Abstract

The differences between the full and shallow-water wave theories for edge waves are reviewed. Detailed comparisons between the solutions of the second-order mass transport velocities within the laminar boundary layer obtained through the two theories are carried out for the first three edge-wave modes. The results clearly show that the error of the shallow-water approximation is larger as the mode number gets larger, and/or the beach slope gets steeper. It is also found that the magnitude of shallow-water approximation error increases in the offshore direction first, then it decreases as the distance approaches further offshore due to the energy decay in that direction. The affecting area of the shallow water approximation is relatively larger for the longshore transport than for the cross-shore transport in higher-mode edge waves. The significant differences between the full and shallow water-wave solutions in the near shore region identified in the present study issue a warning to the modellers of coastal hydrodynamics and nearshore topography, who utilize the shallow water approximation.

Introduction

Edge waves, the waves trapped near the shoreline on a uniformly sloping beach due to wave refraction, were discovered by Stokes (1846). The crest of Stokes' edge wave on a plane beach is perpendicular to the shoreline, it propagates along the shore with the wave amplitude decaying exponentially offshore. Other edge wave modes, besides the Stokes mode, were found by Eckart (1951) through the shallow water-wave theory and Ursell (1952) through the full water wave theory.

[1] Associate Dean, Assistant Professor, Faculty of Science and Technology, University of Macau, PO Box 3001, Macau.
[2] Professor, Box 352700, Dept. of Civil Engr., University of Washington, Seattle, WA 98195, USA

The assumptions associated with the full water wave theory are inviscid and homogeneous fluid, irrotational fluid motion, constant pressure on the free surface, negligible surface tension effect, and only gravity as the restoring force. For the shallow-water wave theory, the assumptions are the same as the full water theory with further simplification; the vertical fluid acceleration is neglected which means that the pressure variation with depth within the fluid domain is hydrostatic, and the horizontal component of the velocity field is uniform over the whole depth. With these assumptions, the problem formulated with the shallow water approximation is reduced to two-dimensional by the depth-integration. The mathematical descriptions of a mode-n progressive edge wave through the shallow water theory (Eckart, 1951) are

$$\phi_s = \frac{a_n g\beta}{\omega}\exp(-k_n y')L_n(2k_n y')\sin(k_n x-\omega t), \tag{1}$$

$$\eta_s = a_n\beta\exp(-k_n y')L_n(2k_n y')\cos(k_n x-\omega t), \tag{2}$$

with the dispersion relation,

$$\omega^2 = gk_n(2n+1)\beta, \tag{3}$$

where n is a non-negative integer (n = 0, 1, 2, 3, ...) representing the offshore mode number, (x, y', z) are the Cartesian coordinates of the alongshore, horizontally offshore and vertically upward directions (the shoreline is at y' = 0 and z = 0), ϕ is the velocity potential, η is the displacement of the water surface from the equilibrium position, a_n is the wave run-up amplitude on the beach, β is the beach sloping angle from the horizontal, ω (= 2π/wave period) is the angular frequency and k (= 2π/wavelength) is the wavenumber in the longshore direction, and $L_n(\bullet)$ is the Laguerre polynomial of order n, which is defined as

$$L_n(s) = \frac{e^s}{n!}\frac{d^n}{ds^n}\left(e^{-s}s^n\right). \tag{4}$$

The counter parts of (1) to (3) by the full water wave theory (Ursell 1952) are

$$\phi = \frac{\alpha_n g}{\omega}\Big[\exp(-k_n y'\cos\beta + k_n z\sin\beta) + \sum_{m=1}^{n} A_{mn}\Big\{\exp\big[-k_n y'\cos(2m-1)\beta - k_n z\sin(2m-1)\beta\big] + \exp\big[-k_n y'\cos(2m+1)\beta + k_n z\sin(2m+1)\beta\big]\Big\}\Big]\sin(k_n x-\omega t), \tag{5}$$

$$\eta = \alpha_n\Big[\exp(-k_n y'\cos\beta) + \sum_{m=1}^{n} A_{mn}\Big\{\exp\big[-k_n y'\cos(2m-1)\beta\big] + \exp\big[-k_n y'\cos(2m+1)\beta\big]\Big\}\Big]\cos(k_n x-\omega t), \tag{6}$$

where

$$A_{mn} = (-1)^m\prod_{j=1}^{m}\frac{\tan(n-j+1)\beta}{\tan(n+j)\beta}, \tag{7}$$

and α_n is a constant. The corresponding dispersion relation is given by

$$\omega^2 = gk_n \sin(2n+1)\beta \tag{8}$$

Ursell (1952) further showed that the number of possible trapped modes depends upon the beach sloping angle β with the maximum mode number n (a non-negative integer) satisfying

$$(2n+1)\beta \le \frac{\pi}{2}. \tag{9}$$

Stokes mode which is also called the mode 0 corresponds to $n = 0$, and edge waves with $n \ge 1$ are termed higher-mode edge waves. It is noted that Eckart's (1951) solution does not give any limitation to the value of the mode number n for a given beach slope; i.e. one cannot distinguish between the trapped modes and those that radiate energy offshore; as $n \to \infty$, the shallow-water wave solution corresponds to the perfectly reflected cross-shore wave (Whitham, 1976) which is obviously not a (trapped) edge-wave mode. To show the discrepancies between the full water-wave solution and the shallow-water wave approximation, Yeh (1986) plotted the surface profiles obtained by the two theories for the first three modes ($n = 0, 1, 2$) on a beach of 15° ($\beta = \pi/12$) slope as shown in figure 1. He showed that the full water-wave and the shallow-water wave solutions have good agreement for the mode-0 edge wave, but the two solutions deviate from each other as either n or y' increases; these deviations reflect the failure of the shallow-water wave

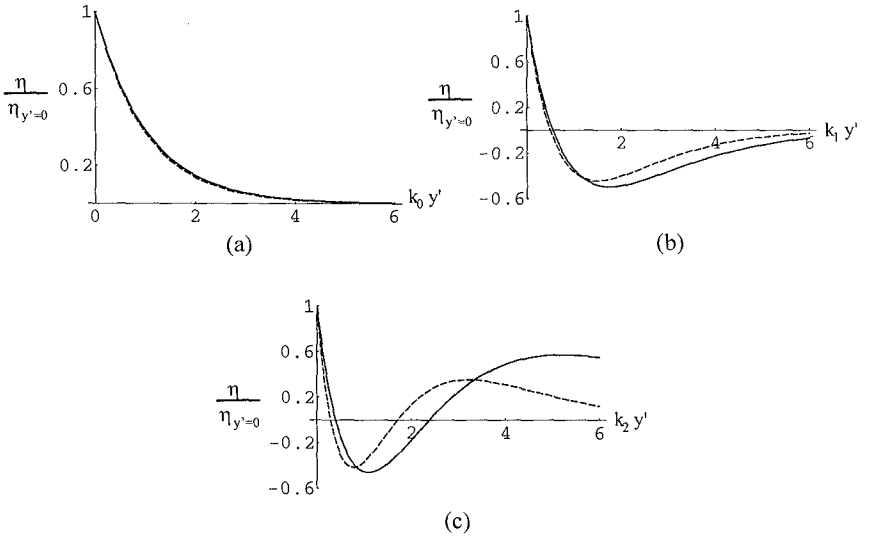

Figure 1. Offshore surface profiles of various edge-wave modes with $\beta = \pi/12$; (a) $n = 0$, (b) $n = 1$, (c) $n = 2$. ——— full theory; ---------- shallow-water approximation.

approximation as $y' \to \infty$ (in deep water). A more general comparison of the water-surface profiles predicted by the full water-wave solution and the shallow water-wave approximation can be demonstrated qualitatively by plotting the normalized difference ε for a range of beach slope and offshore distance;

$$\varepsilon = \frac{\eta_s}{\eta_{s,\, y'=0}} - \frac{\eta}{\eta_{y'=0}}. \tag{10}$$

Figure 2 shows the difference ε for the mode-0, mode-1 and mode-2 edge waves. It is noted that the plot range of the beach slope β is determined by (9). The $\varepsilon = 0$ plane represents the perfect agreement between the two theories. It is clearly shown that the deviation of ε from the zero plane increases both with the beach slope and the mode number. These deviations indicate the failure of the shallow water approximation in deep water. Quantitative comparison of the water surface as shown in figure 2 is given by Mok (1995b) who plotted the contour maps of the difference ε for the mode-0, 1, and 2 edge waves.

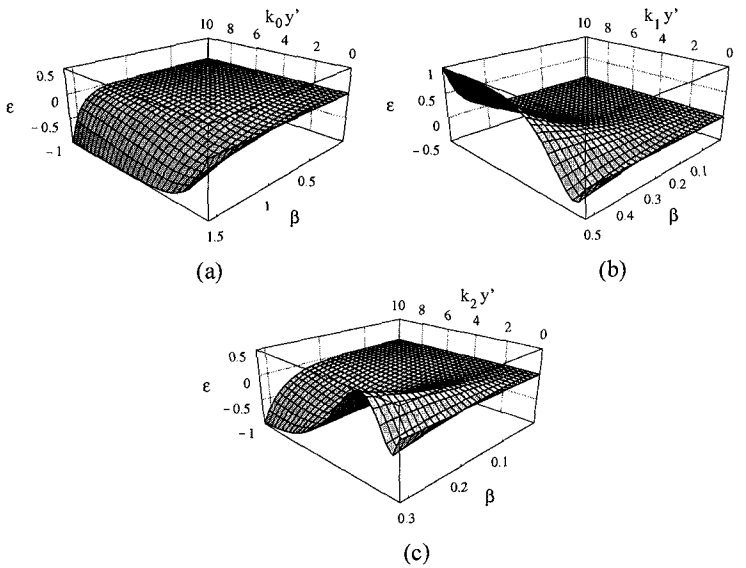

Figure 2. Differences on the water-surface elevation between the full water-wave theory and the shallow-water wave approximation for the (a) mode-0, (b) mode-1, (c) mode-2 edge waves.

In the natural beach environment, various field observations show that edge waves with the mode number less than 5 could be significant nearshore (Munk, Snodgrass & Gilbert, 1964; Huntley & Bowen, 1973; Huntley, 1976; Huntley, Guza & Thornton, 1981; Oltman-Shay & Guza, 1986). Due to the rhythmic characteristics of edge waves in the longshore direction, they can be related to many nearshore morphological features such as the formation of systematically spaced rip currents, nearshore circulation (Bowen & Inman, 1969), crescentic bars, some rhythmic topographical patterns nearshore (Bowen & Inman, 1971; Holman & Bowen, 1982), and beach cusps (Bowen & Inman, 1971; Guza & Inman, 1975; Huntley & Bowen, 1978; Guza & Bowen, 1981). The effects of edge wave on the coastal topography are due to its time-averaged Lagrangian mass-transport velocities (wave induced currents). Even if the magnitude of the induced current might be small, incipience of sediment detachments from the bottom might be caused by the disturbance such as turbulence induced by wave breaking. Then, the fate of the detached sediments might be controlled by the minute-but-persistent time-averaged wave induced currents, and eventually change the sea-bed topography.

Due to simplicity, many of the previous edge-wave mass-transport models (e.g. Bowen & Inman (1971) and Holman & Bowen (1982)) are based on the shallow-water wave theory and the transport velocity is evaluated only at the outer edge of the boundary layer. The question remained is "How much error will the shallow-water approximation introduce to the mass-transport velocity?". In the present study, the second-order mass-transport velocity at the outer edge of the bottom laminar boundary layer derived based on the full water-wave theory is compared with that obtained by the shallow-water-wave theory to identify the differences.

Mass Transport at the Outer Edge of the Bottom Boundary Layer

According to the thin laminar boundary layer theory, the flow field within the bottom viscous layer is driven by the outer irrotational oscillatory flow which is described by the velocity potential. A comparison between (1) and (5) shows that the shallow water solution has the vertical (z-direction) structure of the irrotational flow field removed due to the depth integration operation. This approximation is acceptable when the beach slope or the mode number is small as the vertical structure of the flow field depends on the sine of these two parameters (see (5)). Nevertheless, when the beach slope or the mode number becomes large, the failure of the shallow water approximation is apparent. When the shallow water approximation introduces error into the forcing (the outer irrotational flow field) of the bottom boundary layer, it will pass the error down to the induced second-order mass transport velocity.

Using the full water-wave solution of the velocity potential (5) with the coordinates rotated by the beach slope β,

$$\phi = \frac{\alpha_n g}{\omega}\Big\{\exp(-k_n y) + 2\sum_{m=1}^{n} A_{mn}\exp\left[-k_n y\cos(2m\beta)\right]\cosh\left[k_n z\sin(2m\beta)\right]\Big\}\sin(k_n x - \omega t), \quad (11)$$

Mok & Yeh (1998) and Mok (1992) derived the second-order mass-transport velocity within the thin laminar bottom boundary layer for all modes of progressive edge waves propagating along a uniformly sloping beach. Their solutions are evaluated at the outer edge of the boundary layer here to give the longshore and cross-shore mass-transport velocities ($\overline{u}_L$, $\overline{v}_L$),

$$\overline{u_L} = (\alpha_n g)^2\left(\frac{k_n}{\omega}\right)^3\left\{\frac{3}{2}\left[\exp(-k_n y) + 2\sum_{m=1}^{n} A_{mn}\exp[-k_n y\cos(2m\beta)]\right]\cdot\left[\sum_{m=1}^{n} A_{mn}\sin^2(2m\beta)\exp[-k_n y\cos(2m\beta)]\right] + \frac{1}{2}\left[\left(\exp(-k_n y) + 2\sum_{m=1}^{n} A_{mn}\exp[-k_n y\cos(2m\beta)]\right)^2 + \left(\exp(-k_n y) + 2\sum_{m=1}^{n} A_{mn}\cos(2m\beta)\exp[-k_n y\cos(2m\beta)]\right)^2\right]\right\}, \quad (12)$$

$$\overline{v_L} = -(\alpha_n g)^2\left(\frac{k_n}{\omega}\right)^3\left\{\exp(-k_n y) + 2\sum_{m=1}^{n} A_{mn}\cos(2m\beta)\exp[-k_n y\cos(2m\beta)]\right\}\cdot\left\{-\frac{1}{2}\left[\exp(-k_n y) + \sum_{m=1}^{n} A_{mn}[1+\cos^2(2m\beta)]\exp[-k_n y\cos(2m\beta)]\right] + \left[\sum_{m=1}^{n} A_{mn}\sin^2(2m\beta)\exp[-k_n y\cos(2m\beta)]\right]\right\}, \quad (13)$$

where, the coordinates (x, y, z) are measured longshore, offshore along the bottom and perpendicular to the beach. Based on the mass-transport velocity solutions at the outer edge of the boundary layer given by Hunt & Johns (1963) and the velocity potential given in (1), the second-order mass-transport velocity for progressive edge waves can also be estimated by the shallow-water wave theory. The mass-transport velocities in the longshore and cross-shore directions are, respectively,

$$\overline{u_{L_s}} = (a_n g\beta)^2\left(\frac{k_n}{\omega}\right)^3\frac{1}{4}\Big\{5\exp(-k_n y')[L_n(2k_n y')]^2 - \frac{3}{k_n^2}\exp(-k_n y')L_n(2k_n y')\frac{d^2}{dy'^2}[\exp(-k_n y')L_n(2k_n y')]$$

$$+\frac{2}{k_n^2}\left(\frac{d}{dy'}[\exp(-k_n y')L_n(2k_n y')]\right)^2\Big\}, \tag{14}$$

$$\overline{v_{L_S}} = (a_n g\beta)^2\left(\frac{k_n}{\omega}\right)^3 \frac{1}{4k_n}\frac{d}{dy'}[\exp(-k_n y')L_n(2k_n y')]\cdot$$

$$\Big\{\exp(-k_n y')L_n(2k_n y') - \frac{3}{k_n^2}\frac{d^2}{dy'^2}[\exp(-k_n y')L_n(2k_n y')]\Big\}. \tag{15}$$

Comparison between the Full and Shallow-Water Wave Solutions

Since the coordinate y' for the shallow-water wave solution is measured horizontally offshore and the coordinate y for the full water-wave solution is along the beach bottom, the mass-transport velocities calculated by the shallow-water wave solution are evaluated at position y' but plotted against the corresponding y location ($y = y'/\cos\beta$) in order to be compared with the full water-wave solution. To show the characteristics of the longshore and cross-shore mass transport velocities of progressive edge waves and to be consistent with Yeh's (1986) comparison, the mass-transport velocity profiles obtained by the two theories on a beach of $\pi/12$ slope is plotted to view the differences. The $\beta = \pi/12$ selection restricts the discussions only on the mode-0, mode-1 and mode-2 edge waves according to (9). For both longshore and cross-shore mass-transport velocities of a mode-0 edge wave, the full and shallow-water wave solutions agree with each other (the differences are indistinguishable so that the results are not presented). However, as the mode number becomes larger, the differences appear. Figure 3 shows the longshore and cross-shore mass-transport velocities of a mode-1 edge wave, respectively. It is shown that the differences between the full and shallow-water wave solutions are small. For the longshore transport (figure 3a), the shallow-water wave solution is slightly larger at $k_1 y < 1.68$ and smaller at $k_1 y > 1.68$ than the full water-wave solution. For the cross-shore transport (figure 3b), the two solutions agrees qualitatively. The main differences between them are the locations of the zero mass-transport (zero-crossing) and the offshore locations of the local minimum and maximum. In general, the locations of the zero-transport, local minimum and local maximum predicted by the shallow-water wave theory occur closer to the shore than those predicted by the full water-wave theory. Figure 4 shows the longshore and cross-shore mass-transport velocities of a mode-2 edge wave, respectively. The differences between the full and shallow-water wave solutions are evident. The main differences are the offshore locations of the local minima, local maxima and zero crossings; the shallow-water wave theory still predicts those locations closer to the shore than the full water-wave theory does.

Further general comparisons between the two theories are carried out for the longshore and cross-shore mass transport velocities by plotting the normalized difference

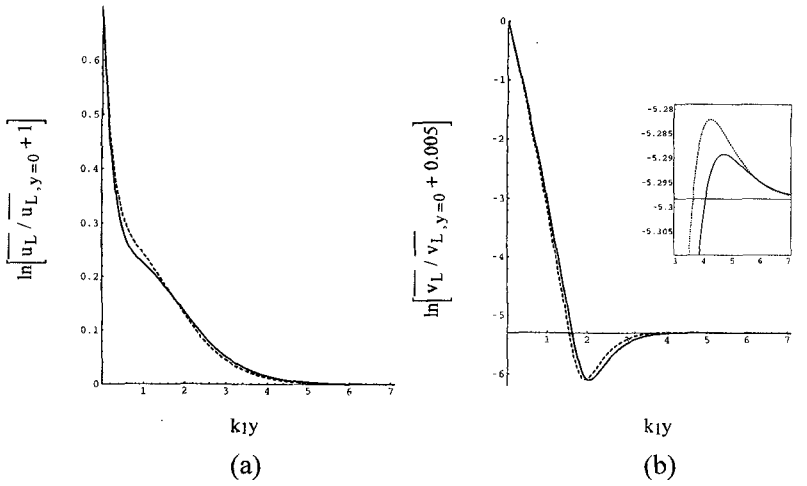

Figure 3. Mass-transport velocity at the outer edge of the boundary layer of a mode-1 progressive edge wave with $\beta = \pi/12$. ——— is the full water-wave solution; ---------- is the shallow-water wave solution. (a) Longshore component, (b) Cross-shore component.

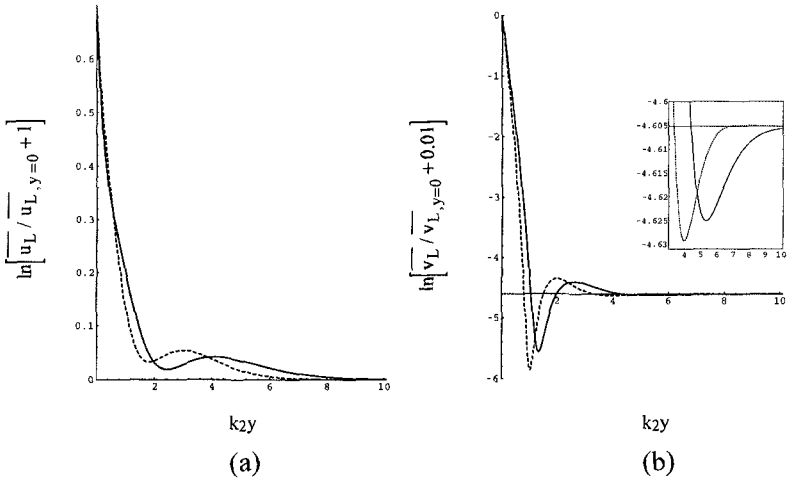

Figure 4. Mass-transport velocity at the outer edge of the boundary layer of a mode-2 progressive edge wave with $\beta = \pi/12$. ——— is the full water-wave solution; ---------- is the shallow-water wave solution. (a) Longshore component, (b) Cross-shore component.

Δu_L and Δv_L for a range of beach slope and offshore distance;

$$\Delta u_L = \frac{\overline{u_{L_s}}}{u_{L_s,y=0}} - \frac{\overline{u_L}}{u_{L,y=0}}, \tag{16}$$

$$\Delta v_L = \frac{\overline{v_{L_s}}}{v_{L_s,y=0}} - \frac{\overline{v_L}}{v_{L,y=0}}. \tag{17}$$

The comparison scheme is to assume that both of the solutions have the same magnitude at the shoreline and see how they deviate from each other as the beach slope and the offshore distance increase. Figure 5 shows the differences Δu_L and Δv_L for a mode-0 edge wave. It is noted that the error chart is valid for both the longshore and cross-shore transports due to the similar offshore structure that they possess. Each line in figure 5 represents the longshore (or cross-shore) transport difference between the two solutions (full and shallow) on beaches of various slope β. For a given beach slope, the magnitude of the error increases offshore from zero to a local maximum then it decreases. The increase of error in the offshore direction at location near the shore reflects the failure of the shallow water approximation due to the increasing water depth. The maximum error of a mode-0 edge wave occurs at $k_0 y < 0.5$ for the entire range of beach slope ($\beta \leq \pi/2$).

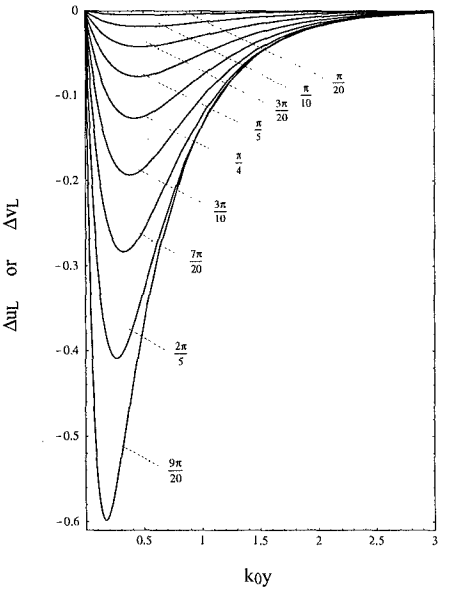

Figure 5. Error chart of the longshore (or cross-shore) transport between the full and shallow-water wave theories for a mode-0 edge wave on various beach slopes.

The decrease of the relative error at further offshore location is due to energy decay in that direction; i.e. the magnitude of the mass-transport velocity is small at location far offshore due to the exponential decay and therefore the relative error between the two solutions becomes small there. On the other hand, the relative error between the two solutions increases with the increasing beach slope for a given offshore location k_0y. This characteristic clearly indicates the effects of the water depth. As the water depth at a fixed offshore location becomes larger with the larger beach slope, the error of the shallow water approximation becomes larger. In fact, this behaviour is expected to be the same for the other edge-wave mode and will not be addressed again in the following discussions for the higher-mode edge waves.

For a mode-1 edge wave, the variation of the error for longshore and cross-shore transports differs. Figure 6 shows the longshore-transport difference Δu_L of a mode-1 edge wave. For the shown beach-slope range, the errors increase offshore from zero to local maxima at $0.5 < k_1y < 0.8$, then it decreases offshore to local minima at $2.0 < k_1y < 2.7$. The magnitudes of the local maxima are larger (about 1.7 times for the case of $\beta = \pi/6$) than the local minima. Nevertheless the magnitude of the error decreases gradually at $k_1y > 2.7$. Again, the increase of error in the offshore direction at location near the shore reflects the failure of the shallow water approximation due to the increasing water

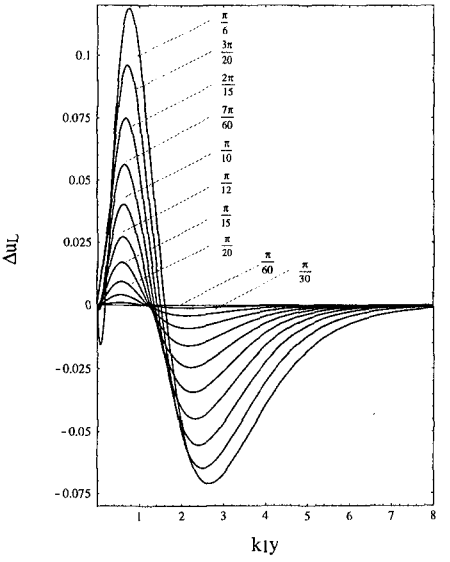

Figure 6. Error chart of the longshore transport between the full and shallow-water wave theories for a mode-1 edge wave on various beach slopes.

depth while the decrease of error at location further offshore ($k_1y > 2.7$) is due to the energy decay as discussed earlier. For the cross-shore mass transport comparison, figure 7 shows the difference Δv_L for a mode-1 wave. Similar to the longshore transport, the magnitudes of the cross-shore transport errors increase in the offshore direction with formation of local minima and maxima at $0.1 < k_1y < 0.2$ and $2.2 < k_1y < 3.0$, respectively. However, the magnitudes of the local minima are much larger (about 7 times for the case of $\beta = \pi/6$) than the local maxima. This significant magnitude difference is caused by the rapid decay of the cross-shore transport velocity in the offshore direction (see figure 3b). Comparing the longshore and cross-shore transport error variation (figures 6, 7), it is clear that the error introduced by the shallow water approximation has a relatively wider offshore coverage for the longshore transport than for the cross-shore transport. Again this is due to the different offshore energy decaying rates of the two transport velocities as shown in figure 3. Note that the complexity of the offshore variation and the existence of local maxima, minima and zero crossings are due to the intersection of the two solutions at various offshore locations (see figure 3).

For the mode-2 edge wave, variation of the error is similar to that of a mode-1 edge wave qualitatively but with more complexity. Detailed description of the comparison is not given for the mode-2 edge wave. Figures 8 and 9 show the longshore-

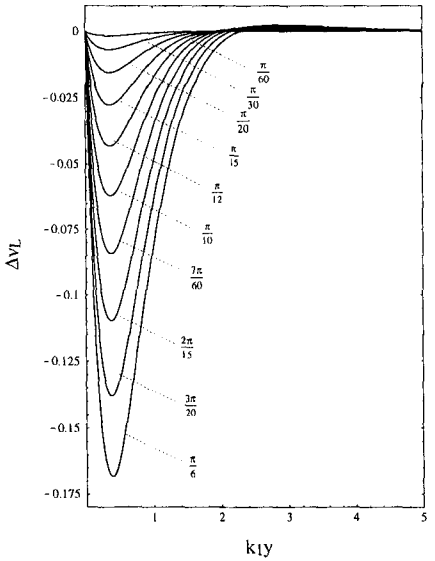

Figure 7. Error chart of the cross-shore transport between the full and shallow-water wave theories for a mode-1 edge wave on various beach slopes.

transport difference Δu_L and the cross-shore transport difference Δv_L for a mode-2 edge wave, respectively. Generally, the error still increases with the beach slope and the offshore distance and forms local maxima and minima. The affecting area of the shallow water approximation is still larger for the longshore transport than for the cross-shore transport.

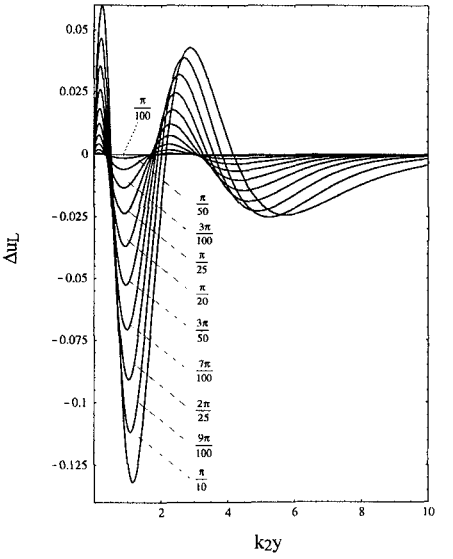

Figure 8. Error chart of the longshore transport between the full and shallow-water wave theories for a mode-2 edge wave on various beach slopes.

Conclusions

Due to its simplicity, many edge-wave mass-transport models are based on the shallow-water approximation. The use of the shallow-water approximation seems reasonable if the beach slope is mild, or only relatively low-mode edge waves are considered. The present study shows that the significant differences between the full and shallow water-wave solutions as the beach slope gets steeper, the distance is farther from the shoreline, or the mode number gets larger issue a warning to the modellers of coastal hydrodynamics and nearshore topography, who utilize the shallow water approximation. Even the present comparison of the two solutions are carried out for mass transport located at the outer part of the boundary layer, it should be noted that there may be major drawbacks on the usage of the mass transport velocity at this location to model the nearshore topography formation. According to Mok's (1995a) experimental verification

and discussions on Dore's (1975) mass transport solution for the Stokes progressive edge wave, the cross-shore transport is bidirectional; the transport is in the inshore direction near the bottom of the boundary layer, while it is in the offshore direction in the upper part of the boundary layer. Evidently, using only the mass-transport velocity at the outer edge of the boundary layer may give an incomplete picture or even misleading prediction of the edge waves' influences on the coastal regions.

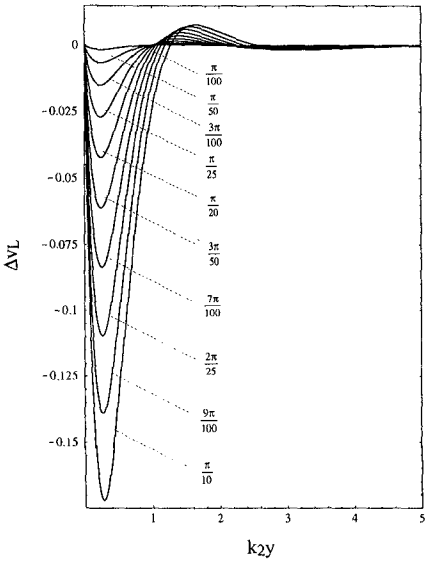

Figure 9. Error chart of the cross-shore transport between the full and shallow-water wave theories for a mode-2 edge wave on various beach slopes.

Acknowledgements

The work for this paper was supported by the US Office of Naval Research (N00014-87-K-0815). The preparation and publication fee of this paper is kindly supported by the University of Macau and the Fundação Oriente.

References

Bowen, A. J. and Inman, D. L. (1969). "Rip-currents: 2. Laboratory and field observations." J. Geophys. Res., 74, 5479-5490.

Bowen, A. J. and Inman, D. L. (1971). "Edge waves and crescentic bars." J. Geophys. Res., 76, 8662-8671.

Dore, B. D. (1975). "Wave-induced vorticity in free-surface boundary layers: application to mass transport in edge waves." J. Fluid Mech., 70, 257-266.

Eckart, C. (1951). "Surface waves on water of variable depth." Wave Report No. 100, Univ. of Calif., Scripps Institution of Oceanography, Calif.

Guza, R. T. and Bowen, A. J. (1981). "On the amplitude of beach cusps." J. Geophys. Res., 86, 4125-4132.

Guza, R. T. and Inman, D. L. (1975). "Edge waves and Beach Cusps." J. Geophys. Res., 80, 2997-3012.

Holman, R. A. and Bowen, A. J. (1982). "Bars, bumps, and holes: models for the generation of complex beach topography." J. Geophys. Res., 87, 457-468.

Hunt, J. N. and Johns, B. (1963). "Currents induced by tides and gravity waves." Tellus, 15, 343-351.

Huntley, D. A. (1976). "Long-period waves on a natural beach." J. Geophys. Res., 36, 6441-6449.

Huntley, D. A. and Bowen, A. J. (1973). "Field observations of edge waves." Nature, 243, 160-162.

Huntley, D. A. and Bowen, A. J. (1978). "Beach cusps and edge waves." Proc., 10th Int. Conf. on Coastal Engrg., 1378-1393.

Huntley, D. A., Guza, R. T. and Thornton, E. B. (1981). "Field observations of surf beat: 1. Progressive edge waves." J. Geophys. Res., 86, 6451-6466.

Mok, K. M. (1992). "Higher-mode edge waves." Ph.D. thesis, Univ. of Wash., Seattle, Wash.

Mok, K. M. (1995a). "An experimental study on mass transport of progressive Stokes edge waves." Proc., XXVI IAHR Congress, London, UK, 3, 186-191.

Mok, K. M., (1995b). "Edge waves - the differences between the full and shallow water-wave theories." Proc., 17th Conf. on Ocean Engrg. and 1995 Cross-Strait Conf. on Port and Coastal Development, Tainan, Taiwan, 1, 393-405.

Mok, K. M., and Yeh, H. (1998). "On mass transport of progressive edge waves." In Preparation.

Munk, W., Snodgrass, F. and Gilbert, F. (1964). "Long waves on the continental shelf: an experiment to separate trapped and leaky modes." J. Fluid Mech., 20, 529-554.

Oltman-Shay, J. and Guza, R. T. (1986). "Infragravity edge wave observations on two California beaches." J. Phys. Oceanogr., 17, 644-663.

Stokes, G. G. (1846). "Report on recent researches in hydrodynamics." Rep. 16th meeting Brit. Assoc. Adv. Sci., 1-20 = Math. Physics Papers, 1, 157-187, Cambridge, 1880.

Ursell, F. (1952). "Edge waves on a sloping beach." Proc., R. Soc. Lond. A, 214, 79-97.

Whitham, G. B. (1976). "Nonlinear effects in edge waves." J. Fluid Mech., 74, 353-368.

Yeh, H. H. (1986). "Experimental study of standing edge waves." J. Fluid Mech., 168, 291-304.